AperTO - Archivio Istituzionale Open Access dell'Università di Torino

Modelled phototransformation kinetics of the antibiotic sulfadiazine in organic matter-rich lakes

This is the author's manuscript

Original Citation:

Availability:

This version is available http://hdl.handle.net/2318/1687091 since 2019-01-17T13:11:21Z

Published version:

DOI:10.1016/j.scitotenv.2018.07.206

Terms of use:

Open Access

Anyone can freely access the full text of works made available as "Open Access". Works made available under a Creative Commons license can be used according to the terms and conditions of said license. Use of all other works requires consent of the right holder (author or publisher) if not exempted from copyright protection by the applicable law.

(Article begins on next page)

08 November 2024

Modelled phototransformation kinetics of the antibiotic sulfadiazine in organic matter-rich lakes

Davide Vione,[a,b]* Birgit Koehler [c]

[a] *Department of Chemistry, University of Torino, Via Pietro Giuria 5, 10125 Torino, Italy*

[b] *NatRisk Inter-Department Centre, University of Torino, Largo Paolo Braccini 2, 10095 Grugliasco (TO), Italy*

[c] *Department of Ecology and Genetics/Limnology, Evolutionary Biology Centre, Uppsala University, Norbyvägen 18 D, 75236 Uppsala, Sweden*

* Corresponding author. E-mail: *davide.vione@unito.it*

Abstract

Xenobiotic compounds are commonly detected in inland waters. Sunlight-induced photochemical reactions contribute to xenobiotic degradation, but the role of different photoreactions on large geographic scales remains poorly understood. Here, we used a combination of photochemical modelling and large-scale field data from 1020 lakes across Sweden to elucidate the photodegradation kinetics of the commonly used antibiotic sulfadiazine (SDZ) in organic matter-rich lakes. SDZ occurs in two forms, namely acidic HSDZ (pK_a = 6.5) and basic/deprotonated SDZ^-. Both species are oxidised fast by the photogenerated triplet states of natural organic matter ($^3NOM^*$). However, they also undergo efficient back reactions because the partially oxidised HSDZ (and SDZ^- to a larger extent) can be reduced back to the initial compounds by the phenolic moieties contained in NOM. Typical lakes in Sweden are rich in NOM and have low pH, with the consequence that SDZ photochemistry would be dominated by HSDZ. Our simulation results

showed that SDZ photodegradation kinetics in Swedish lakes would become significantly slower with increasing water depth and pH, while it depended little on latitude, which affects irradiance, or on organic matter content. As a consequence, SDZ would be particularly persistent in lakewater in some densely populated areas with relatively deep and high-pH lakes such as, most notably, the Stockholm region. Here the surface waters could be more heavily contaminated by pharmaceuticals compared to the scarcely populated regions in the centre-north of the country, where lakewater could otherwise promote an efficient photodegradation of SDZ.

Keywords: sulfonamides; surface-water photochemistry; triplet sensitisation; natural organic matter; back reactions.

Introduction

Human activities, such as the production and use of medical drugs, pesticides, herbicides or plastics, contribute to the pollution of inland waters (Boethling et al., 2009). Among the contaminants of emerging concern there is sulfadiazine (SDZ), a sulfonamide antibiotic that is widely applied in the treatment of urinary tract infections, bacterial encephalitis, toxoplasmosis, malaria, and against bacterial infections that may arise in the HIV disease (NIH, 2017). The incomplete removal of SDZ in urban wastewater treatment plants (Kümmerer, 2009; Altunok et al., 2016; Li et al., 2016; Sun et al., 2016) accounts for its emissions into surface water bodies, which also takes place because of the SDZ extensive use in livestock husbandry (Kasteel et al., 2010) and fish aquaculture (Almeida et al., 2011). SDZ has thus been detected worldwide, at concentration levels ranging from a few ng L^{-1} up to μg L^{-1} in Europe, Asia and North America (Kolpin et al., 2002; Hollender et al., 2009; Yang et al., 2011). SDZ is a weak acid that can occur in two main forms in natural waters, namely the acidic, undissociated HSDZ and the basic, deprotonated SDZ^{-} (Lin et al., 1997; Sanli et al., 2010). Hereafter, SDZ will refer to the overall compound (sum of HSDZ and SDZ^{-}), while the two different species will be indicated as HSDZ and SDZ^{-}.

It is important to understand the degradation pathways of pollutants in different aquatic systems and on large scales (Fenner et al., 2013). Wastewater treatment plants mainly rely on biological (activated sludge) degradation to remove nutrients (Polesel et al., 2016), but the SDZ antibiotic properties are unfavourable to bacterial degradation (Li and Zhang, 2011; Huang et al., 2016). The biorecalcitrant nature of SDZ during wastewater treatment may be reflected in slow biodegradation in the natural environment (Adamek et al., 2016), but biorecalcitrant compounds in activated sludge may actually biodegrade in natural aquatic systems due to differences in microbial community composition (Fono et al., 2006; Kunkel and Radke, 2011). Overall, the biological lifetime of SDZ in surface-water environments in temperate regions is in the range of 20-30 days (Adamek et al., 2016). The other important transformation pathway in sunlit surface waters is photodegradation, which takes place by direct photolysis and indirect photochemistry (Boreen et al., 2003; Remucal, 2014; Koehler et al., 2018). SDZ photodegradation was competitive with SDZ biodegradation in a wide range of summertime environmental conditions (Wenk and Canonica, 2012; Bahnmüller et al., 2014).

Direct photolysis follows photon absorption, and it is enabled by the fact that both HSDZ and SDZ^{-} absorb sunlight at $\lambda < 400$ nm. The direct photolysis of sulfonamide antibiotics such as SDZ proceeds either via photochemical sulfur dioxide (SO_2) extrusion (also observed in the case of indirect photochemistry; Boreen et al., 2005), or via addition of a hydroxy group (OH; Challis et al., 2013). The latter probably does not involve hydroxyl radicals ($^{\bullet}OH$), but follows photoionisation and reaction of the radical cation with water, plus deprotonation and hydrogen detachment by O_2

(Gligorovski et al., 2015). In the case of SDZ, SO_2 photoextrusion might significantly increase the toxicity of the reaction product towards crustaceans (e.g., daphnids; Mayo-Bean et al., 2012).

Indirect photochemistry is triggered upon photon absorption by natural water constituents that act as photosensitisers, such as natural organic matter (NOM), nitrate and nitrite ions (Boreen et al., 2003). Indirect photochemistry involves reactive species such as $^{\bullet}OH$, the carbonate radical ($CO_3^{\bullet-}$), natural organic matter triplet states ($^3NOM^*$) and singlet oxygen ($^1O_2$) (Vione et al., 2014; Rosario-Ortiz and Canonica, 2016; McNeill and Canonica, 2016). The main environmental factors regulating SDZ photodegradation are the water depth, pH and TOC (total organic carbon) concentration (note that TOC is a measure of NOM) (Vione et al., 2018). HSDZ is mainly phototransformed upon reaction with $^{\bullet}OH$ in low-TOC waters, and by direct photolysis and $^3NOM^*$ oxidation in intermediate to high-TOC waters. Direct photolysis is more important for SDZ^- than for HSDZ, while in both cases the reaction with $^1O_2$ is hardly significant (Vione et al., 2018).

The SDZ + $^3NOM^*$ reactions are interesting because the primary process is relatively fast. However, the radical species arising from the oxidation of HSDZ and SDZ^- by $^3NOM^*$ are promptly reduced back to the primary compounds by the NOM anti-oxidant moieties (Wenk and Canonica, 2012; Bahnmüller et al., 2014). Because organic matter can both enhance (via $^3NOM^*$) and inhibit (via back-reduction; Canonica and Laubscher, 2008) the degradation of SDZ, it is interesting to assess the expected SDZ behaviour in high-TOC waters. Such waters often occur at elevated latitudes in the boreal hemisphere, and boreal lakes are usually very NOM-rich compared to lakes in temperate or tropical regions (Sobek et al., 2007). However, even though sulfonamide antibiotics occur in boreal freshwater environments (Zou et al., 2015a/b), the photodegradation of SDZ under these conditions has not yet been assessed. Moreover, the NOM-concentration of many boreal lakes is increasing due to a combination of recovery from acidification, increased precipitation and related soil runoff, the latter being most likely connected with climate change

(Solomon et al., 2015; Weyhenmeyer et al., 2016). There is evidence that these environments are favourable to photochemical reactions (Koehler et al., 2014), and particularly to those induced by ^{3}NOM* (Koehler et al., 2018).

An earlier study has suggested that despite back reduction, the relative importance in HSDZ/SDZ^{-} degradation of ^{3}NOM* compared to other photoreactions should increase with increasing TOC, at least up to about 10 mg_C L^{-1} (Vione et al., 2018). However, estimates of SDZ phototransformation kinetics for higher TOC values are currently unavailable. SDZ is the only compound that is known to undergo the back-reduction process, for which a modelling exercise of this kind is possible at the present state of knowledge, because of the availability of ^{3}NOM* reaction rate constants and of back-reaction parameters (Vione et al., 2018). Therefore, this study has the goal of assessing the phototransformation kinetics and pathways of SDZ in waters that are rich in organic matter, such as those found in Swedish lakes.

Materials and Methods

Simulation of the pathways of SDZ phototransformation

SDZ undergoes photodegradation by direct photolysis, and by indirect photochemistry via reactions with $^{\bullet}OH$, $^3NOM^*$ and $^1O_2$ (Vione et al., 2018). The radical $^{\bullet}OH$ is produced upon sunlight irradiation of NOM, nitrate and nitrite, and it is consumed by reaction with NOM, bicarbonate and carbonate (Vione et al., 2014). The transient family $^3NOM^*$ is produced by NOM following radiation absorption and inter-system crossing, and it is mainly scavenged by dissolved O_2 (partially to produce $^1O_2$) and by internal conversion. The lifetime of $^3NOM^*$ in anoxic waters is an order of magnitude longer than in oxygenated systems (McNeill and Canonica, 2016). There is also an additional process of $^3NOM^*$ scavenging by NOM, which can only be important in NOM-rich environments (Wenk et al., 2013). Finally, $^1O_2$ is produced by reaction between $^3NOM^*$ and O_2 and it is scavenged by collision with water (Vione et al., 2014). Generally, low-TOC environments are favourable to the processes induced by $^{\bullet}OH$. In contrast, intermediate-TOC waters favour direct photolysis, and high-TOC systems best trigger $^3NOM^*$ and $^1O_2$ reactions (Vione et al., 2014). The actual photodegradation pathway(s) followed by a given substrate depend as well on its intrinsic reactivity towards the different photoprocesses (Boreen et al., 2003).

We carried out a preliminary study of the main SDZ phototransformation pathways by using the software APEX (Aqueous Photochemistry of Environmentally-occurring Xenobiotics; Bodrato and Vione, 2014). To date, the relevant pathways are only available for the 0-10 $mg_C\ L^{-1}$ organic carbon range (Vione et al., 2018). This range may be suitable for temperate water bodies, but is definitely below the TOC concentrations often found in boreal lakes. Therefore, we extended the model simulations up to 100 mg_C L^{-1}, thereby covering a large TOC variability that is representative of boreal environments (Sobek et al., 2007).

APEX uses as input data the photoreactivity parameters of the substrate, which in the present case are referred to HSDZ or SDZ^- (absorption spectra, direct photolysis quantum yields, and second-order reaction rate constants with $^{\bullet}OH$, $^3NOM^*$ and $^1O_2$), as well as environmental parameters connected with photoreactivity. HSDZ and SDZ^- react in a similar way (no significant pH trend reported) with both $^{\bullet}OH$ (rate constant of 3.7×10^9 L mol^{-1} s^{-1}) and $^1O_2$ (rate constant of 8.9×10^6 L mol^{-1} s^{-1}) (Boreen et al., 2005). The second-order reaction rate constants of HSDZ and SDZ^- with the triplet state of the NOM proxy 4-carboxybenzophenone are $k^o_{HSDZ,^3NOM^*}$ = 4.9×10^9 and $k^o_{SDZ^-,^3NOM^*}$ = 2.9×10^9 L mol^{-1} s^{-1} (Li et al., 2015). However, the primary oxidised radical species are efficiently reduced back to HSDZ/SDZ^- by the phenolic NOM moieties (Canonica and Laubscher, 2008). The back-reduction process is enhanced with increasing TOC, so that the apparent second-order reaction rate constant between x = HSDZ or SDZ^- and $^3NOM^*$ can be expressed as follows (Wenk et al., 2011):

$$k_{x,^3NOM^*} = k^o_{x,^3NOM^*} \frac{1}{1+\dfrac{TOC}{TOC_{1/2}}} \quad (1)$$

where $TOC_{1/2}$ is the TOC value for which $k_{x,^3NOM^*}$ is halved compared to $k^o_{x,^3NOM^*}$. In the case of HSDZ/SDZ^-, the best estimates for $TOC_{1/2}$ are 17 mg_C L^{-1} (HSDZ) and 0.7 mg_C L^{-1} (SDZ^-) (Vione et al., 2018). The needed modification in the APEX code to include **Eq. (1)** was implemented as described in Vione et al. (2018). The effect of the TOC on the value of $k_{x,^3NOM^*}$ is reported in

Figure 1a for both HSDZ and SDZ^-. It is clear that the back reduction is more important in the case of SDZ^-, probably because the oxidation of HSDZ and SDZ^- by $^3NOM^*$ yields different radical species (Tentscher et al., 2013), having different back-reduction kinetics in the presence of NOM anti-oxidants. Because such radical species might be involved in acid-base equilibria, not dissimilarly from the parent compounds HSDZ/SDZ^-, this explanation implies that back reduction be faster than protonation-deprotonation (Vione et al., 2018).

Key environmental data used by APEX include water depth, absorption spectrum (largely accounted for by NOM), chemical composition, and the quantum yields of $^\bullet OH$, $^1O_2$ and $^3NOM^*$ photoproduction by irradiated NOM. Typical water depth, absorbance and chemistry data for Swedish lakes were available from the 2009 Swedish National Lake Inventory by the Swedish University of Agricultural Sciences (Erlandsson et al., 2012, Koehler et al., 2014). The NOM quantum yield values used in the present work to describe the photogeneration of reactive transients ($\Phi_{^\bullet OH}^{NOM}$ = 3×10^{-5}, $\Phi_{^1O_2}^{NOM}$ = 1.2×10^{-3}, $\Phi_{^3NOM^*}^{NOM}$ = 1.3×10^{-3}) have proven suitable to predict the photodegradation kinetics of the xenobiotics carbamazepine and ibuprofen in two lakes located in Southern Sweden, namely Lake Boren and Norra Bergundasjön (Koehler et al., 2018). Due to the elevated TOC values involved in the present simulation, the scavenging of $^3NOM^*$ by NOM was taken into account by considering the second-order rate constant $k_{NOM,^3NOM^*}$ = 1.7×10^3 L mg_C^{-1} s^{-1} (Wenk et al., 2013), in addition to k' = 5×10^5 s^{-1} that is the decay constant of $^3NOM^*$ in aerated solution (McNeill and Canonica, 2016). APEX assumes well-mixed waters, thus the photoreaction kinetics data obtained in relatively deep lakes depend on the contributions of the well-illuminated and highly photoreactive surface layer, and of the dark and poorly photoreactive lower depths (Bodrato and Vione, 2014).

The standard solar spectrum used in APEX is reported in **Figure 1b**, together with the absorption spectra of both HSDZ and SDZ^{-} (Vione et al., 2018). The sunlight spectrum is referred to a solar zenith angle of 40°, which can be found for instance at mid-latitude (45°N) on 15 July, at 9 am or 3 pm solar time. At 55°N, the latitude of the southernmost studied lakes, the same conditions occur on 15 July at 9.30 am or 2.30 pm, while in Central Sweden (65°N) they are reached at noon on the summer solstice.

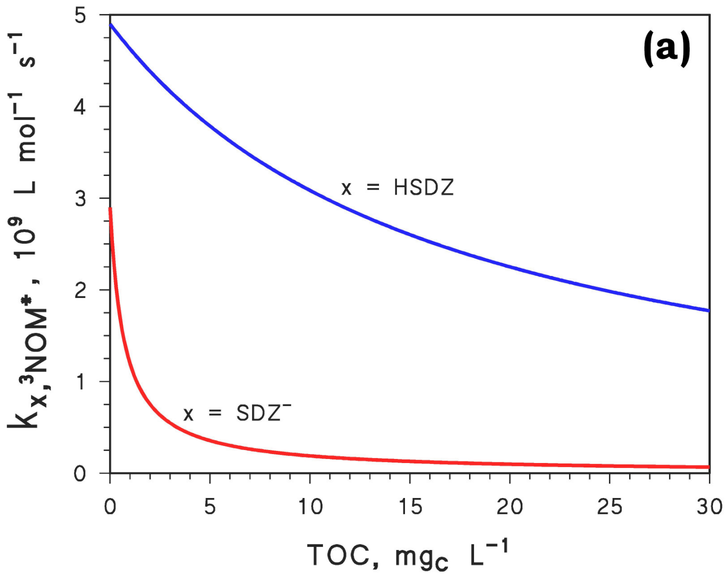

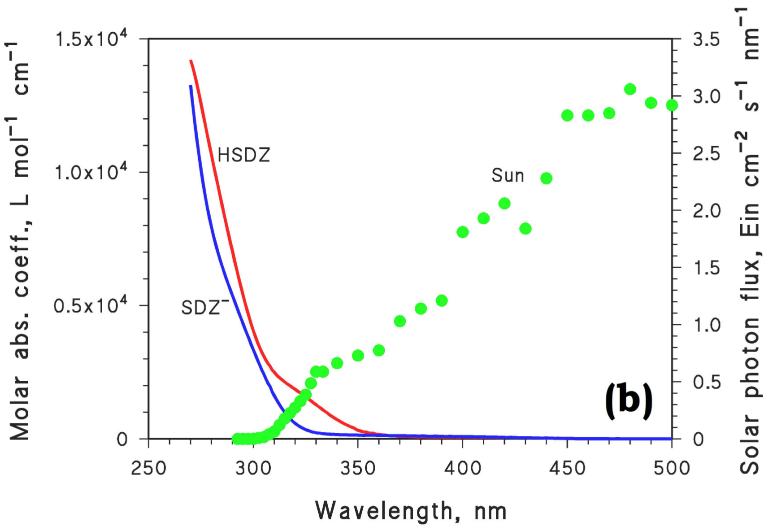

Figure 1. (a) TOC trends of $k_{x,^3NOM^*}$ according to **Eq. (1)**, for x = HSDZ ($TOC_{1/2}$ = 17 mg$_C$ L^{-1}) and x = SDZ^- ($TOC_{1/2}$ = 0.7 mg$_C$ L^{-1}).

(b) Left Y-axis: absorption spectra (molar absorption coefficients) of HSDZ and SDZ^-. Right Y-axis: spectral photon flux density of fair-weather sunlight (45°N: 15 July at 9 am or 3 pm, 1 April or 7 September at noon; 55°N: 15 July at 9.30 am or 2.30 pm, 30 April or 15 August at noon; 65°N: 21 June at noon).

Simulation of SDZ phototransformation kinetics across Swedish lakes

The assessment of SDZ phototransformation kinetics in the boreal study lakes was carried out with a methodology similar to that used in the APEX simulations, but included some peculiarities that are not easily implemented within the APEX code for a 1020-lake dataset. Briefly, we used the following approach: *(i)* calculation of the photon fluxes absorbed by HSDZ, SDZ^-, NOM and nitrate in a water column, the depth of which was equal to the average depth of each lake (nitrite was often undetectable, and in any case NOM is by far the main $^\bullet OH$ source in Swedish lakes; Koehler et al., 2018); *(ii)* calculation, on the basis of photon absorption, of the direct photolysis rates of HSDZ/SDZ^- and of the formation rates/steady-state concentrations of $^\bullet OH$, $^1O_2$ and $^3NOM^*$; *(iii)* determination of the first-order rate constants and half-life times of HSDZ/SDZ^- (and of SDZ at the lakewater pH value), both in the separate photoprocesses and as a whole, due to all photoreactions; *(iv)* mapping of the relevant half-life times across the Swedish lakes under study. The different procedures are now explained in more detail.

The photon flux absorbed by NOM was calculated for Sep 22, 2009 (autumnal equinox during the year of lake water sampling) for wavelengths of 280 to 600 nm (1-nm resolution) from the surface of each lake in 0.005-m-increments down to the average lake depth z_{ave}, as follows:

$$P_a^{NOM} = \int_0^{z_{ave}} \int_{\lambda_{\min}}^{\lambda_{\max}} E_{od}^{Day}(\lambda,-0)\, a_g(\lambda)\; e^{-(K_d(\lambda)\, z)}\, d\lambda\, dz \qquad (2)$$

where z is depth (m), λ_{min} = 280 nm, λ_{max} = 600 nm, $E_{od}^{Day}(\lambda,-0)$ is the daily-integrated-downwelling scalar irradiation just below the water surface (mol photons m^{-2} day^{-1} nm^{-1}), a_g is the NOM Napierian absorption coefficient (m^{-1}, calculated from measured NOM absorbance; Koehler et al., 2014) and K_d is the vertical attenuation coefficient for downward irradiance (m^{-1}, estimated using regression relationships from literature data and data fit with an exponential function to obtain continuous spectra; Koehler et al., 2014).

The solar spectrum $E_{od}^{Day}(\lambda,-0)$ was simulated as described in detail earlier (Koehler et al. 2014). Briefly, we first used the atmospheric radiative transfer model libRadtran 1.6 (Mayer et al., 2011) to obtain hourly clear-sky downwelling spectra of global and diffuse irradiance reaching the water-air interface. The clear-sky irradiance spectra were corrected for attenuation by clouds using a cloud effect function (Kasten et al., 1980), based on UV irradiance measurements from Norrköping, Sweden (year 2008, n=2400), and cloud cover data from the archive of the operational mesoscale analysis system MESAN at the Swedish Meteorological and Hydrological Institute (Hāggmark et al., 2000). Subsequently, transmittance of the cloud-corrected above-water-surface irradiance across the air-water interface was calculated separately for the diffuse and direct fraction. The just below-water-surface hourly diffuse and direct downwelling irradiance spectra were converted to scalar irradiance spectra, and integrated to obtain daily irradiation spectra.

The photon flux absorbed by nitrate was calculated as follows:

$$P_a^{NO_3^-} = \int_0^{z_{ave}} \int_{\lambda_{\min}}^{\lambda_{\max}} \frac{\varepsilon_{NO_3^-}(\lambda)\ C_{NO_3^-}}{a_g(\lambda)}\ E_{od}^{Day}(\lambda,-0)\ a_g(\lambda)\ e^{-(K_d(\lambda)z)}\ d\lambda\, dz \tag{3}$$

where $\varepsilon_{NO_3^-}$ is the molar absorption coefficient of nitrate (L μg N^{-1} m^{-1}) and $c_{NO_3^-}$ is nitrate concentration (μg N L^{-1}). The photon flux absorbed by x = HSDZ or SDZ$^-$, with concentration [x] (mol L^{-1}), was calculated as follows (Koehler et al., 2018):

$$P_a^x = [x]\int_0^{z_{ave}} \int_{\lambda_{min}}^{\lambda_{max}} \frac{\varepsilon_x(\lambda)}{a_g(\lambda)} \cdot E_{od}^{Day}(\lambda,-0)\; a_g(\lambda)\; e^{-(K_d(\lambda)z)}\, d\lambda\, dz \qquad (4)$$

where $\varepsilon_x(\lambda)$ is the molar absorption coefficient (L mol^{-1} cm^{-1}). The concentration [x] should be assumed as low enough, so that radiation absorption by x does not affect the absorption by the other water components. To this purpose, we used [x] = 10^{-8} mol L^{-1} but the model results would not be affected by either increasing or decreasing this concentration value by two orders of magnitude. The absorbed photon fluxes were transformed in units of mol photons L^{-1} s^{-1}, and the formation rates of $^{\bullet}$OH, ^{3}NOM* and $^1O_2$ as well as the direct photolysis (d.p.) decay kinetics of HSDZ/SDZ$^-$ (units of mol L^{-1} s^{-1}) were calculated as follows:

$$R_{^{\bullet}OH} = R_{^{\bullet}OH}^{NOM} + R_{^{\bullet}OH}^{NO_3^-} = \Phi_{^{\bullet}OH}^{NOM}\; P_a^{NOM} + \Phi_{^{\bullet}OH}^{NO_3^-}\; P_a^{NO_3^-} \qquad (5)$$

$$R_{^3NOM^*} = \Phi_{^3NOM^*}^{NOM}\; P_a^{NOM} \qquad (6)$$

$$R_{^1O_2} = \Phi_{^1O_2}^{NOM}\; P_a^{NOM} \qquad (7)$$

$$R_x^{d.p.} = \Phi_x\, P_a^S \qquad (8)$$

where $\Phi_{^{\bullet}OH}^{NO_3^-}$ = 0.01 (Warneck and Wurzinger, 1988), Φ_{HSDZ} = 0.4×10^{-3} and Φ_{SDZ^-} = 1.2×10^{-3} (Boreen et al., 2005). The steady-state concentrations of $^{\bullet}$OH, ^{3}NOM* and $^1O_2$ (mol L^{-1}) were determined as the ratio between the relevant formation rates and the pseudo-first order decay (or scavenging) rate constants, as follows:

$$[^{\bullet}OH] = \frac{R_{^{\bullet}OH}}{k_{NOM,^{\bullet}OH}\, TOC + k_{HCO_3^-,^{\bullet}OH}\,[HCO_3^-] + k_{CO_3^{2-},^{\bullet}OH}\,[CO_3^{2-}]} \qquad (9)$$

$$[^3NOM^*] = \frac{R_{^3NOM^*}}{k' + k_{NOM,^3NOM^*}\,TOC} \qquad (10)$$

$$[^1O_2] = \frac{R_{^1O_2}}{k_d} \qquad (11)$$

where $k_{NOM,^{\bullet}OH}$ = 2×10^4 L mg_C^{-1} s^{-1} (Brezonik and Fulkerson-Brekken, 1998), $k_{HCO_3^-,^{\bullet}OH}$ = 8.5×10^6 L mol^{-1} s^{-1} (Buxton et al., 1988), $k_{CO_3^{2-},^{\bullet}OH}$ = 3.9×10^8 L mol^{-1} s^{-1} (Buxton et al., 1988), k' = 5×10^5 s^{-1} (McNeill and Canonica, 2016), $k_{NOM,^3NOM^*}$ = 1.7×10^3 L mg_C^{-1} s^{-1} (Wenk et al., 2013), and k_d = 2.5×10^5 s^{-1} (Wilkinson and Brummer, 1981).

It follows the reactions of HSDZ/SDZ^- with $^{\bullet}OH$, $^3NOM^*$ and $^1O_2$, for which we used the same rate constant values already mentioned in the framework of the APEX simulations. On this basis, the first-order degradation rate constant k_x (s^{-1}) and the half-life time $t_{1/2}^x$ (units of s, then converted into more manageable time units) were expressed as follows (x = HSDZ or SDZ^-, as usual):

$$k_x = \frac{R_x^{d.p.}}{[S]} + k_{x,^{\bullet}OH}[^{\bullet}OH] + k_{x,^3NOM^*}[^3NOM^*] + k_{x,^1O_2}[^1O_2] \qquad (12)$$

$$t_{1/2}^x = \frac{\ln 2}{k_x} \qquad (13)$$

In particular, note that $k_{x,^3NOM^*}$ is described by **Eq. (1)**. The overall rate constant of SDZ (HSDZ + SDZ^-) phototransformation was calculated by taking into account the acid-base equilibrium HSDZ $\leftrightarrows$ SDZ^- + H^+, which has acidic dissociation constant pK_a = 6.5 (Lin et al., 1997; Sanli et al., 2010):

$$k_{SDZ} = \frac{[H^+]}{[H^+] + K_a} k_{HSDZ} + \frac{K_a}{[H^+] + K_a} k_{SDZ^-} \quad (14)$$

The $[H^+]$ values were obtained from the reported pH of the water of each relevant lake. Note that lakes in Sweden are usually more acidic compared to temperate regions, due to relatively low alkalinity (Erlandsson et al., 2012). Typical water-chemistry conditions for Swedish lakes are reported in **Table 1**. Moreover, we used $t_{1/2}^{SDZ} = \ln 2\,(k_{SDZ})^{-1}$ to derive half-life times from the first-order degradation rate constants. On this basis, colour-coded maps visualising patterns across the Swedish lakes were produced using the Sweden *rds* file provided in the Database of Global Administrative Areas (GADM) 2015 (http://gadm.org/country) and the software R version 3.4.2 (R.D.C. Team, 2017).

Table 1. Water ionic composition across the study lakes (data from the Swedish National Lake Inventory 2009, downloaded from the "Data host for inland waters" from the Swedish University of Agricultural Sciences (http://info1.ma.slu.se/ri/www_ri.acgi$Project?ID=2009KS, last accessed July 2018).

Characteristic	Mean ± SE	Range	Median	Interquartile Range
Conductivity (mS m^{-1})	6.51 ± 0.62	0.28 – 569.00	3.70	2.12 – 7.00
Alcalinity/Acidity (meq L^{-1})	0.27 ± 0.02	-0.32 - 4.64	0.14	0.05 - 0.27
Nitrate (μg N L^{-1})	44.15 ± 3.91	1.00 - 2880	15.00	3.00 - 44.75
Chloride (meq L^{-1})	0.18 ± 0.05	0.003 – 45.88	0.06	0.02 - 0.20
Sulfate (meq L^{-1})	0.09 ± 0.01	0.002 - 5.63	0.04	0.02 – 0.10
Fluoride (mg L^{-1})	0.14 ± 0.004	0.02 - 0.88	0.10	0.06 - 0.18
Calcium (meq L^{-1})	0.31 ± 0.02	0.003 – 5.32	0.17	0.10 – 0.32
Magnesium (meq L^{-1})	0.11 ± 0.01	0.004 - 9.16	0.07	0.04 - 0.11
Sodium (meq L^{-1})	0.19 ± 0.04	0.004 - 36.70	0.08	0.05 - 0.21
Potassium (meq L^{-1})	0.02 ± 0.001	0.001 - 0.97	0.01	0.01 - 0.02

Results and discussion

Simulation of the pathways of SDZ phototransformation

For photochemistry in high-TOC waters one should consider the possible scavenging of ^{3}NOM* by NOM. The results of the simulations (steady-state [^{3}NOM*] with varying TOC and water depth, with sunlight irradiance corresponding to mid-latitude 15 July at 9 am or 3 pm solar time) are reported in **Figure 2a**. The comparison between the values of [^{3}NOM*] obtained upon consideration of the NOM scavenging, or by neglecting it, suggests that the scavenging process becomes significant above 20 $mg_C\ L^{-1}$ TOC. At 100 $mg_C\ L^{-1}$ TOC, which is near the upper limit of this parameter for surface-water environments (Wetzel, 2001), the scavenging decreases [^{3}NOM*] by around 25%. Understandably, as shown in the figure, [^{3}NOM*] is higher in shallow (1 m) than in deeper waters (5-10 m). In the latter, the contribution of the well-illuminated (high-[^{3}NOM*]) surface layer is offset by the darker lower depths (low-[^{3}NOM*]; Bodrato and Vione, 2014).

The [^{3}NOM*] trend reported above has some impact on the phototransformation of HSDZ, as shown in **Figure 2b** that compares the predicted photodegradation kinetics (first-order degradation rate constant k_{HSDZ}), with and without NOM scavenging. It is interesting to observe that the scavenging of ^{3}NOM* by NOM slows down the photodegradation of HSDZ at high TOC by approximately the same extent as it decreases [^{3}NOM*]. This means that ^{3}NOM* should play a major role in HSDZ photodegradation at high TOC, which is confirmed by the plot of the model-predicted HSDZ phototransformation pathways as a function of the TOC (**Figure 3a**). According to this plot, the $^\bullet$OH reaction and the direct photolysis would be the main HSDZ pathways for TOC < 5 $mg_C\ L^{-1}$, while ^{3}NOM* would predominate above that TOC value. The trend curve of k_{HSDZ} vs. TOC for water depth d = 1 m (**Figure 2b**) is remarkable because of the "step" between 5 and 10

$mg_C\ L^{-1}$. A compound undergoing photodegradation by $^{\bullet}OH$/direct photolysis at low TOC and by $^3NOM^*$ at high TOC, but without the back-reduction effect of NOM anti-oxidant moieties, would show a minimum in the *k* vs. TOC curve (Calza et al., 2017). This happens because the scavenging of $^{\bullet}OH$ by NOM, and the inhibition by NOM itself of the compound direct photolysis (because of competition for sunlight irradiance) account for the initial decrease of *k* vs. TOC. On the other hand, [$^3NOM^*$] increases with increasing TOC and photodegradation becomes faster again as the $^3NOM^*$ pathway gains importance, which produces the minimum. However, in the case of HSDZ the TOC has a further inhibitory effect, i.e. the back-reduction carried out by the NOM anti-oxidant moieties, which offsets the increase of [$^3NOM^*$] with increasing TOC. Moreover, while the anti-oxidant effect becomes progressively more important as the TOC gets higher, [$^3NOM^*$] has a plateau trend with TOC because of absorption saturation and NOM scavenging (Braslavsky, 2007). Therefore, k_{HSDZ} shows a step-like feature followed by a decrease. The "step" becomes less evident as the water depth increases (see the cases of 5 and 10 m vs. 1 m in **Figure 2b**), because in deeper water the saturation of absorption by NOM is reached more easily.

The case of SDZ^- is different because, compared to HSDZ, the $^3NOM^*$-mediated phototransformation undergoes a much higher inhibition by the back reactions, which limits the importance of $^3NOM^*$ at elevated TOC. Therefore, the main SDZ^- phototransformation process is the direct photolysis in a wide range of TOC values (see **Figure 3b**). Because of this, and because the SDZ^- direct photolysis is inhibited at high TOC due to the competition with NOM for sunlight irradiance, the phototransformation rate constant of SDZ^- has a consistent decreasing trend with increasing TOC (see **Figure 2c**).

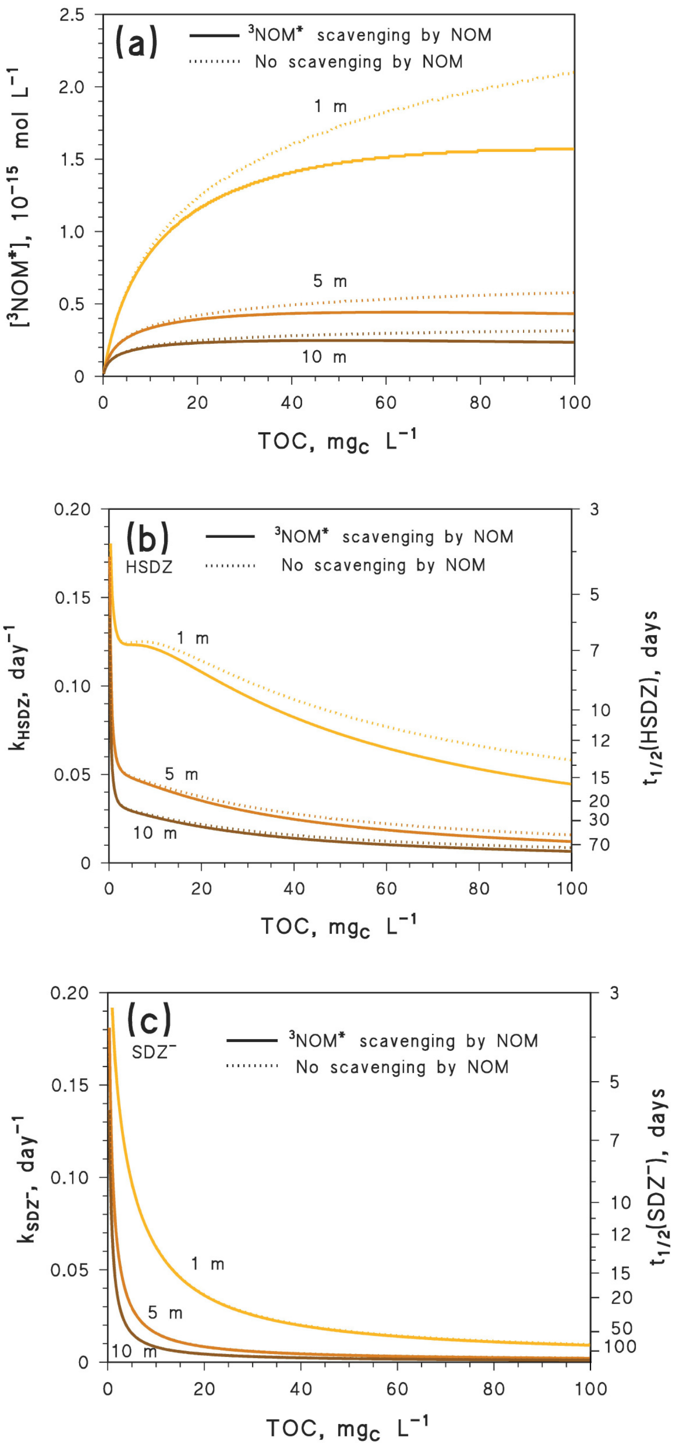

Figure 2. Predicted trend of the steady-state [^{3}NOM*] as a function of the TOC, for depths of the well-mixed water columns of 1, 5 and 10 m, with and without ^{3}NOM* scavenging by NOM **(a)**. Predicted TOC trends of the first-order decay constants k_{HSDZ} **(b)** and k_{SDZ^-} **(c)** for column depths of 1, 5 and 10 m, with and without ^{3}NOM* scavenging by NOM. The corresponding half-life times ($t_{1/2} = \ln 2(k)^{-1}$) are also reported, and the time unit is mid-latitude summer days. Other water conditions: 0.1 mmol L^{-1} nitrate, 1 mmol L^{-1} bicarbonate, 10 μmol L^{-1} carbonate. For **(a)** the steady-state concentrations are referred to 22 W m^{-2} sunlight UV irradiance, corresponding to the spectrum reported in **Figure 1**. Note than in panel **(c)** the solid and dotted curves overlap.

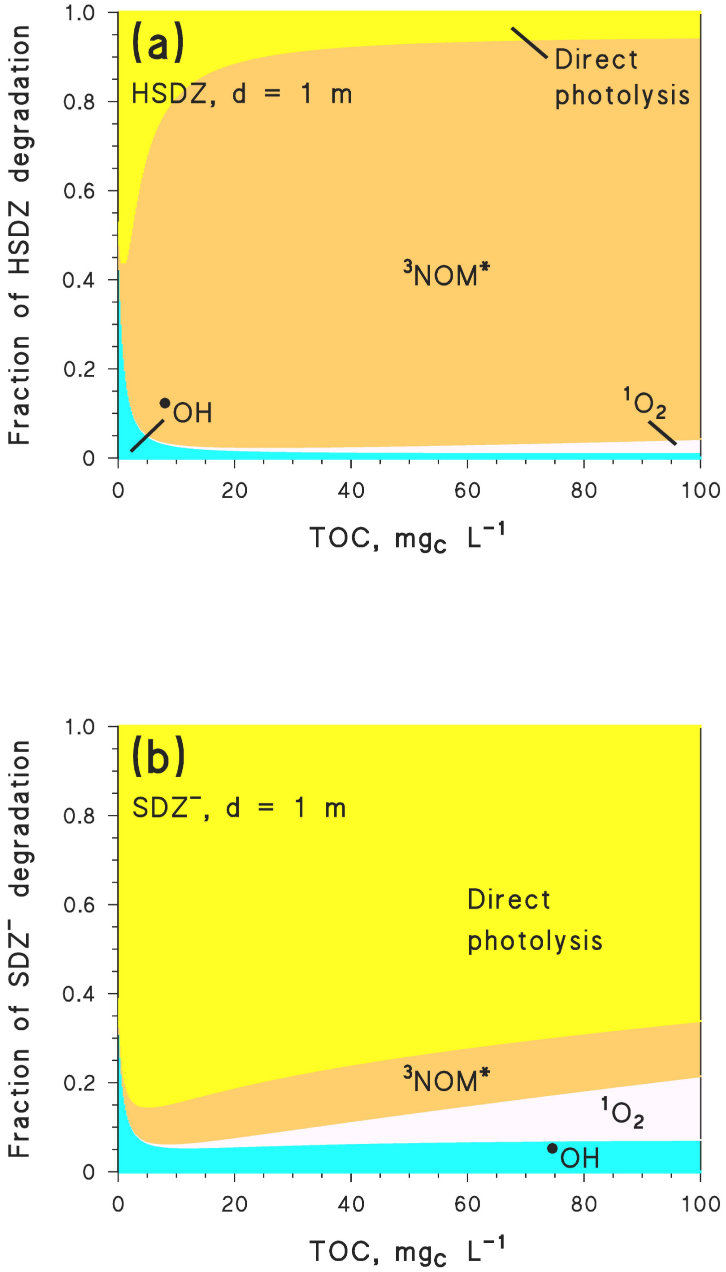

Figure 3. Predicted fractions of HSDZ **(a)** and SDZ^- **(b)** phototransformation accounted for by the different photoprocesses, as a function of the water TOC, for a water column depth of 1 m. Other water conditions, as well as sunlight irradiance and spectrum are the same as for **Figure 2**. The ^{3}NOM* scavenging by NOM was taken into account in these calculations.

The ^{3}NOM* scavenging by NOM has little importance in the case of SDZ^- photodegradation (see the almost perfect overlap between the solid -^{3}NOM* scavenging- and dotted -no scavenging- curves in the figure). Indeed, a 25% decrease in [^{3}NOM*] and, therefore, in the corresponding rate of the ^{3}NOM* reaction would not impact much the overall kinetics of SDZ^- photodegradation (see **Figure 3b**, which shows the limited role that ^{3}NOM* plays in the case of SDZ^-).

Because HSDZ and SDZ^- show different phototransformation kinetics (see **Figure 2**), the water pH is understandably important to determine the rate constants and lifetimes of the photoinduced degradation of SDZ. As shown in **Figure 4**, increasing pH slightly enhances the phototransformation of SDZ at low TOC and significantly inhibits it at high TOC. Coherently with the results of Vione et al. (2018), SDZ^- is slightly more photolabile than HSDZ at low TOC, where the direct photolysis is an important process for both compounds (**Figure 3**). However, SDZ^- becomes considerably less photoactive than HSDZ at high TOC because of the inhibition of direct photolysis, and of the higher importance that the back-reactions play towards ^{3}NOM*-mediated transformation in the case of SDZ^- compared to HSDZ. Indeed, differently from SDZ^-, ^{3}NOM* processes dominate the photochemistry of HSDZ at high TOC (**Figure 3**).

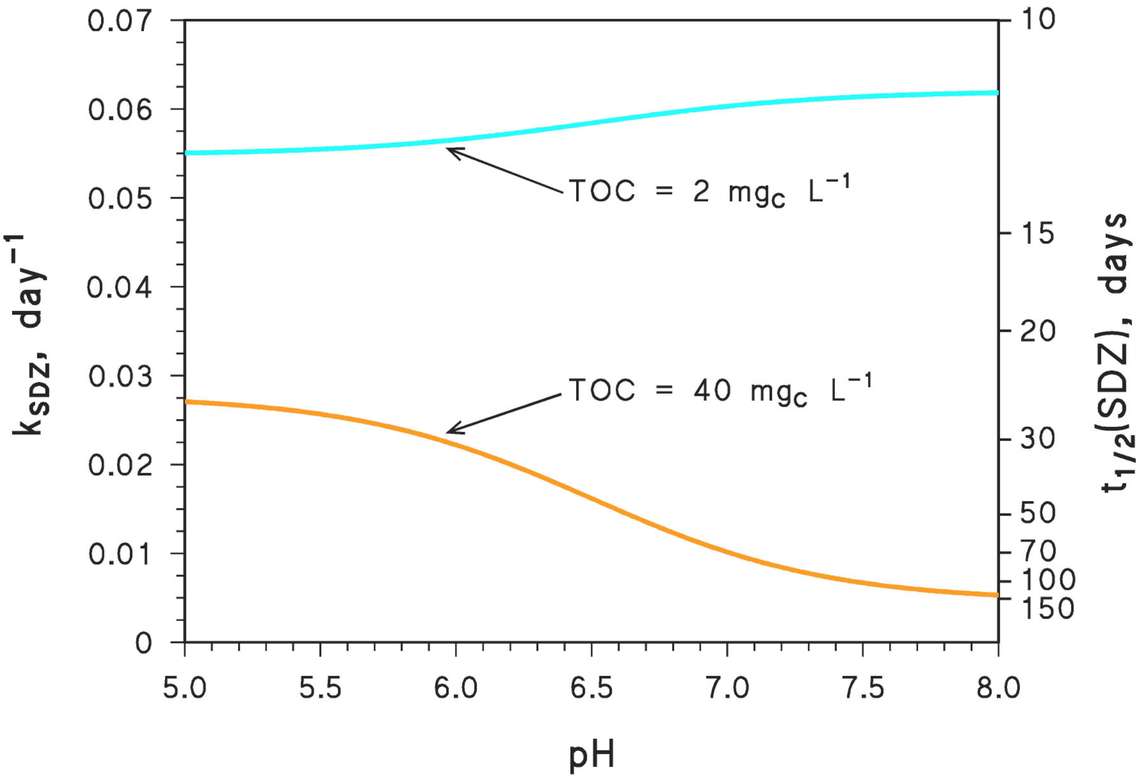

Figure 4. Predicted trends with pH of the first-order decay constant k_{SDZ} and of the corresponding half-life time ($t_{1/2}(SDZ) = \ln 2\,(k_{SDZ})^{-1}$), for TOC values of 2 and 40 mg$_C$ L^{-1}. Other water conditions: 0.1 mmol L^{-1} nitrate, 1 mmol L^{-1} bicarbonate, 10 μmol L^{-1} carbonate, 5 m depth. The time unit is mid-latitude summer days. The ^{3}NOM* scavenging by NOM was taken into account in these calculations.

Simulating SDZ photochemistry across Swedish lakes

Based on data of water chemistry (most notably, pH, nitrate, inorganic carbon and TOC) and depth of over one thousand lakes in Sweden, combined with simulated lake-specific sunlight irradiance and spectrum referred to the fall equinox, we were able to predict the kinetics of SDZ (HSDZ + SDZ^{-}) phototransformation in the lake water. The previous discussion has shown that TOC, water depth and pH are the main lake-related environmental factors that affect the kinetics of SDZ photodegradation. Latitude may also be important, but at least as far as the fall equinox is concerned, water chemistry and depth play a more substantial role (Koehler et al., 2018).

The lakes with the highest NOM content (TOC > 20 mg_C L^{-1}, **Figure 5a**) and the deepest water columns (average depth > 5 m, **Figure 5b**) are often located in Southern Sweden. Interestingly, elevated TOC values and relatively deep waters tend to produce longer photochemical lifetimes for both HSDZ and SDZ^{-} (see **Figure 2**). The pH map of Sweden (**Figure 5c**) is a bit different, because the lakes characterised by relatively high pH values (i.e., > 7) are mostly located in the south and north of the country. In contrast, the most acidic lakes (pH < 5.5) are concentrated in the northern central region, relatively near the Baltic Sea coast (i.e., part of the counties of Västerbotten and Västernorrland). It should be underlined that the Scandinavian region in general and Sweden in particular is generally poor in carbonate rocks, which accounts for the relatively acidic lakewater when compared to several other regions of the world. For the same reason (low buffering capacity of lakewater), in the past many Scandinavian lakes have been subject to significant acidification phenomena caused by acidic depositions from the atmosphere (Futter et al., 2014).

The predicted photochemical lifetimes are reported in **Figure 6** for the cases of HSDZ (**6a**), SDZ^{-} (**6b**) and SDZ (**6c**). First of all, it appears clearly that HSDZ usually undergoes faster degradation compared to SDZ^-, because of the relatively high TOC values that are commonly found in Swedish lakes. The two SDZ species show in fact similar phototransformation kinetics at low TOC, but HSDZ is considerably more photolabile at high TOC (see **Figure 4**). The north-south polarisation that is generally found in TOC (**Figure 5a**) and water depth (**Figure 5b**) is generally maintained in the lifetimes of both HSDZ and SDZ^- (**Figure 6a/b**), which are longer in Southern Sweden but with some peculiarities. A correlation study does in fact suggest that the HSDZ lifetime is directly proportional to the water depth ($R^2 = 0.71$, $n = 1020$, $p < 0.00001$) and poorly dependent on the TOC ($R^2 = 0.002$, $p = 0.96$), while the SDZ^- lifetime shows some positive correlation (statistically significant but with relatively low correlation coefficient) with both depth ($R^2 = 0.24$) and TOC ($R^2 = 0.27$). The reason is that both direct photolysis (degrading SDZ^-) and $^3NOM^*$ reactions (degrading HSDZ) are inhibited in deep water, while the presence of NOM only inhibits the direct photolysis. The $^3NOM^*$ process should be favoured at high TOC, but the back reactions weaken the $^3NOM^*$-TOC correlation as far as SDZ photodegradation is concerned.

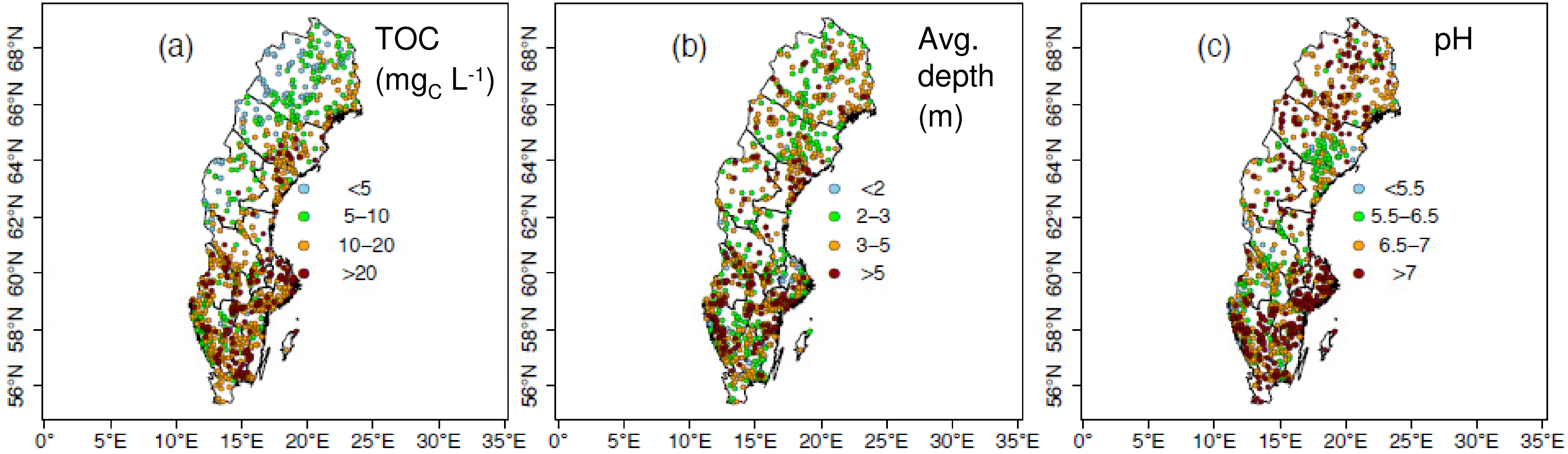

Figure 5. Maps of Sweden showing the location of the 1020 modelling study lakes (circles), colour-coded according to concentration of TOC (a, mg_C L^{-1}), average water depth (b, metres) and water pH (c, pH units). The colour coding of the classes are given in each panel, and the lines denote the counties of Sweden.

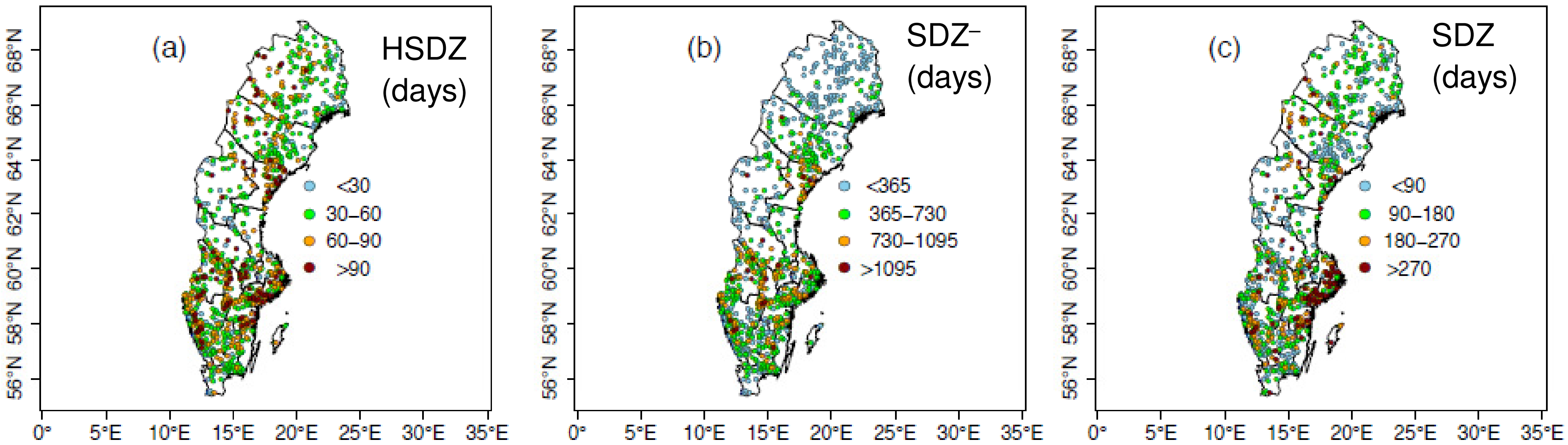

Figure 6. The location of the 1020 modelling study lakes (circles) across Sweden, colour-coded according to the simulated half-life times (days) of (a) HSDZ, (b) SDZ^{-} and (c) SDZ (i.e., HSDZ + SDZ^{-}). The colour coding of the classes are given in each panel. The lines denote the counties of Sweden.

The most important datum is obviously the overall SDZ lifetime (**Figure 6c**), which was directly proportional to the water depth (R^2 = 0.44) and pH (R^2 = 0.31), but unrelated to the TOC (R^2 = 0.04). Photodegradation is expected to be favoured in acidic lakes, because it involves to a larger extent the more photolabile HSDZ species. The lakes showing the longest SDZ lifetimes (> 270 days) are mostly concentrated in the Stockholm region, where the lakes are often relatively deep and with relatively high pH values (**Figure 5**). In contrast, there are several other lakes in Southern Sweden (including the Malmö and Gothenburg areas) where SDZ would be photodegraded rather quickly (lifetime < 3 months) because of the shallow water columns and despite the relatively high pH values. With few exceptions, lakes in Central and Northern Sweden appear to be the most favourable environments to SDZ photodegradation, because of shallow water and, particularly in Västerbotten/Västernorrland, relatively low pH values. Interestingly, the latitudinal gradient of the predicted SDZ photodegradation kinetics (faster in the north and slower in the south) runs counter to the gradient of equinox sunlight irradiance. This means that, in the case of Sweden at the fall equinox, lake water features including depth and pH would be more important than latitude to determine how fast SDZ undergoes photodegradation. The role of latitude may be different when higher irradiance differences are expected, but that applies most notably to the winter season when all photochemical processes are significantly inhibited. During summer, when the higher solar zenith angle in Northern compared to Southern Sweden is offset by the longer daylight hours in the north and photochemistry is most significant, an even smaller latitude-irradiance effect is expected compared to the fall equinox.

Relatively few data exist of the occurrence of SDZ in surface freshwaters of the Scandinavian peninsula (Norden, 2012), although this compound has been detected in sediments of the Baltic Sea (Åland Sea; Hallgren and Wallberg, 2016). Sulfamethoxazole, which belongs to the same class of sulfonamide antibiotics, appears to be ubiquitous in Southern Sweden and its surface-water concentration approaches the $\mu g\ L^{-1}$ level (Norden, 2012). Unfortunately, the photodegradation of sulfamethoxazole cannot be modelled because key data are missing, as they have been recently provided for SDZ only (Vione et al., 2018). However, it has been shown that sulfamethoxazole and SDZ have comparable lifetimes in the presence of NOM under simulated sunlight irradiation (Bahnmüller et al., 2014), and a 1-month lifetime is reported for sulfamethoxazole in Norra Bergundasjön, Southern Sweden (Zou et al., 2015a). This lake has 3.3 m average depth, pH around 6.5 and TOC = 8-10 mg_C L^{-1} (H. Olofsson, unpublished data), under which conditions the photodegradation of HSDZ would be faster than that of SDZ^- (Vione et al., 2018). Based on the Norra Bergundasjön water features at the time of the field study carried out by Zou et al. (2015a), one can assess [$^3NOM^*$] = 0.5-1.5×10^{-16} mol L^{-1} (Koehler et al., 2018) that would provide a SDZ lifetime of 20-50 days. If one tentatively assumes that the photochemical SDZ lifetime can be representative of that of sulfamethoxazole (coherently with data by Bahnmüller et al., 2014, under simulated sunlight), the similarity of the SDZ predictions and the measured field persistence of sulfamethoxazole suggests that photodegradation could be significant for sulfonamide antibiotics in Norra Bergundasjön. Interestingly, the photodegradation of SDZ would be the slowest in one of the most densely populated areas of Sweden (Stockholm region), where the occurrence of sulfonamides in surface waters could be higher compared to the very scarcely populated northern regions (Norden, 2012). In the latter locations one often has a remarkable potential for lake water to degrade SDZ, which is anyway less likely to occur at important concentration levels.

Conclusions

Here, we provide a model assessment of the photodegradation kinetics of sulfadiazine (SDZ, HSDZ + SDZ^-) in NOM-rich (high-TOC) waters. Both HSDZ (pK_a = 6.5) and SDZ^- show high reactivity towards $^3NOM^*$. However, SDZ^- also undergoes very efficient back-reactions triggered by NOM, which do not allow the triplet-sensitised degradation to gain importance as the TOC increases. Indeed, direct photolysis would be the main phototransformation pathway of SDZ^{-} in a wide variety of environmental conditions. In contrast, because of less effective back reactions, triplet sensitisation by NOM would become the main HSDZ photoprocess at TOC concentrations above about 5 mg_C L^{-1} TOC. HSDZ and SDZ^{-} are expected to show similar reactivity in low-TOC environments, while HSDZ would be more photolabile than SDZ^{-} at TOC values above 3 mg_C L^{-1} (Vione et al., 2018). The latter TOC interval encompasses only the NOM-rich temperate lakes (Wetzel, 2001), but the vast majority of boreal ones (Sobek et al., 2007). Therefore, in high-TOC waters one expects the overall SDZ photodegradation to be faster as the pH is lower.

Swedish lakes are a very representative and well-known case of high-TOC waters, where the available information allows for the modelling of SDZ photodegradation kinetics on a wide geographic basis. Under fall-equinox sunlight irradiation conditions the most important environmental factors driving SDZ photodegradation in Swedish lakes appeared to be water depth and pH, while latitude (affecting sunlight irradiance) and the water TOC were less important. Interestingly, the densely populated Stockholm area hosts the majority of the lakes where the SDZ photochemical lifetime is expected to be the slowest (> 270 days). The ability of lakewater to induce SDZ photodegradation would be generally higher in lakes located in other populated areas of Southern Sweden (e.g., Malmö and Gothenburg). Remarkably, SDZ could be photodegraded relatively fast in many lake environments of Central and Northern Sweden, which are characterised by shallow water columns and low pH. However, since these lakes are usually located in very scarcely populated areas, they may not suffer much from contamination by pharmaceuticals.

Acknowledgements

DV acknowledges financial support by University of Torino and Compagnia di San Paolo (project CSTO168282-ABATEPHARM).

References

Adamek, E., Baran, W., Sobczak, A., 2016. Assessment of the biodegradability of selected sulfa drugs in two polluted rivers in Poland: Effects of seasonal variations, accidental contamination, turbidity and salinity. J. Hazard. Mater. 313, 147-158.

Almeida, S. A., Heitor, A. M., Montenegro, M. C., Sales, M. G., 2011. Sulfadiazine-selective determination in aquaculture environment: Selective potentiometric transduction by neutral or charged ionophores. Talanta 85, 1508-1516.

Altunok, M, König, A., Mahmoud Ahmed, W. M. M., Haddad, T., Vasconcelos, T. G., Kümmerer, K., 2016. Automated determination of sulfadiazine in water, fish plasma and muscle by HPLC with on-line column-switching. Clean Soil Air Water 44, 967-974.

Bahnmüller, S., von Gunten, U., Canonica, S., 2014. Sunlight-induced transformation of sulfadiazine and sulfamethoxazole in surface waters and wastewater effluents. Water Res. 57, 183-192.

Bodrato, M., Vione, D., 2014. APEX (Aqueous Photochemistry of Environmentally occurring Xenobiotics): A free software tool to predict the kinetics of photochemical processes in surface waters. Environ. Sci.-Processes Impacts 16, 732–740.

Boethling, R., Fenner, K., Howard, P., Klečka, G., Madsen, T., Snape, J. R., Whelan, M. J., 2009. Environmental persistence of organic pollutants: guidance for development and review of POP risk profiles. Integr. Environ. Assess. Manag. 5, 539-556.

Boreen, A. L., Arnold, W. A., McNeill, K., 2003. Photodegradation of pharmaceuticals in the aquatic environment: A review. Aquat. Sci. 65, 320-341.

Boreen, A. L., Arnold, W. A., McNeill, K., 2005. Triplet-sensitized photodegradation of sulfa drugs containing six-membered heterocyclic groups: Identification of an SO_2 extrusion photoproduct. Environ. Sci. Technol. 39, 3630-3638.

Braslavsky, S.E., 2007. Glossary of terms used in photochemistry, 3rd edition. Pure Appl. Chem. 79, 293-465.

Brezonik, P.L., Fulkerson-Brekken, J., 1998. Nitrate-induced photolysis in natural waters: Controls on concentrations of hydroxyl radical photo-intermediates by natural scavenging agents. Environ. Sci. Technol. 32, 3004-3010.

Buxton, G. V., Greenstock, C. L., Helman, W. P., Ross, A. B., 1988. Critical review of rate constants for reactions of hydrated electrons, hydrogen atoms and hydroxyl radicals ($^{\bullet}OH/^{\bullet}O^{-}$ in aqueous solution. J. Phys. Chem. Ref. Data 17, 513–886.

Calza, P., Noé, G., Fabbri, D., Santoro, V., Minero, C., Vione, D., Medana, C., 2017. Photoinduced transformation of pyridinium-based ionic liquids, and implications for their photochemical behavior in surface waters. Water Res. 122, 194-206.

Canonica, S., Kohn, T., Mac, M., Real, F.J., Wirz, J., Von Gunten, U., 2005. Photosensitizer method to determine rate constants for the reaction of carbonate radical with organic compounds. Environ. Sci. Technol. 39, 9182-9188.

Canonica, S., Laubscher, H.-U., 2008. Inhibitory effect of dissolved organic matter on triplet-induced oxidation of aquatic contaminants. Photochem. Photobiol. Sci. 7, 547-551.

Challis, J. K., Carlson, J. C., Friesen, K. J., Hanson, M. L., Wong, C. S., 2013. Aquatic photochemistry of the sulfonamide antibiotic sulfapyridine. J. Photochem. Photobiol. A: Chem. 262, 14-21.

Erlandsson, M., Futter, M. N., Kothawala, D., Koehler, S. J., 2012. Variability in spectral absorbance metrics across boreal lake waters. J. Environ. Monit. 14, 2643–2652.

Fenner, K., Canonica, S., Wackett, L. P., Elsner, M., 2013. Evaluating pesticide degradation in the environment: blind spots and emerging opportunities. Science 341, 752–758.

Fono, L. J., Kolodziej, E. P., Sedlak, D. L., 2006. Attenuation of wastewater-derived contaminants in an effluent-dominated river. Environ. Sci. Technol. 40, 7257-7262.

Futter, M. N., Valinia, S., Löfgren, S., Köhler, S. J., Fölster, J., 2014. Long-term trends in water chemistry of acid-sensitive Swedish lakes show slow recovery from historic acidification. Ambio 43, 77-90.

Gligorovski, S., Strekowski, R., Barbati, S., Vione, D., 2015. Environmental implications of hydroxyl radicals ($^{\bullet}OH$). Chem. Rev. 115, 13051-13092.

Hāggmark, L., Ivarsson, K. I., Gollvik, S., Olofsson, P. O., 2000. Mesan, an operational mesoscale analysis system. Tellus A 52, 2–20.

Hallgren, P., Wallberg, P., 2015. Background report on pharmaceutical concentrations and effects in the Baltic Sea. Policy Area Hazards of the EU Strategy for the Baltic Sea Region. Swedish Environmental Protection Agency, Stockholm, Sweden.

Hollender, J., Zimmermann, S. G., Koepke, S., Krauss, M., McArdell, C. S., Ort, C., Singer, H., von Gunten, U., Siegrist, H., 2009. Elimination of organic micropollutants in a municipal wastewater treatment plant upgraded with a full-scale post-ozonation followed by sand filtration. Environ. Sci. Technol. 43, 7862-7869.

Huang, X. F., Feng, Y., Hu, C., Xiao, X. Y., Yu, D. L., Zou, X. M., 2016. Mechanistic model for interpreting the toxic effects of sulfonamides on nitrification. J. Hazard. Mater. 305, 123-129.

Kasteel, R., Mboh, C. M., Unold, M., Groeneweg, J., Vanderborght, J., Vereecken, H., 2010. Transformation and sorption of the veterinary antibiotic sulfadiazine in two soils: A short-term batch study. Environ. Sci. Technol. 44, 4651-4657.

Kasten, F., Czeplak, G., 1980. Solar and terrestrial radiation dependent on the amount and type of cloud. Sol. Energy 24, 177−189.

Koehler, B., Landelius, T., Weyhenmeyer, G. A., Machida, N., Tranvik, L. J., 2014. Sunlight-induced carbon dioxide emissions from inland waters. Glob. Biogeochem. Cycle 28, 696–711.

Koehler, B., Barsotti, F., Minella, M., Landelius, T., Minero, C., Tranvik, L. J., Vione, D., 2018. Simulation of photoreactive transients and of photochemical transformation of organic pollutants in sunlit boreal lakes across 14 degrees of latitude: A photochemical mapping of Sweden. Water Res. 129, 94-104.

Kolpin, D. W., Furlong, E. T., Meyer, M. T., Thurman, E. M., Zaugg, S. D., Barber, L. B., Buxton, H. T., 2002. Pharmaceuticals, hormones, and other organic wastewater contaminants in US streams, 1999-2000: A national reconnaissance. Environ. Sci. Technol. 36, 1202-1211.

Kunkel, U., Radke, M., 2011. Reactive tracer test to evaluate the fate of pharmaceuticals in rivers. Environ. Sci. Technol. 45, 6296-6302.

Kümmerer, K., 2009. Antibiotics in the aquatic environment – A review – Part I. Chemosphere 75, 417-434.

Li, B., Zhang, T., 2011. Mass flows and removal of antibiotics in two municipal wastewater treatment plants. Chemosphere 83, 1284-1289.

Li, Y. J., Wei, X. X., Chen, J. W., Xie, H. B., Zhang, Y. N., 2015. Photodegradation mechanism of sulfonamides with excited triplet state dissolved organic matter: A case of sulfadiazine with 4-carboxybenzophenone as a proxy. J. Hazard. Mater. 290, 9-15.

Li, Y. X., Liu, B., Zhang, X. L., Wang, J., Gao, S. Y., 2016. The distribution of veterinary antibiotics in the river system in a livestock-producing region and interactions between different phases. Environ. Sci. Pollut. Res. 23, 16542-16551.

Lin, C. E., Lin, W. C., Chen, Y. C., Wang, S. W., 1997. Migration behavior and selectivity of sulfonamides in capillary electrophoresis. J. Chromatogr. A 792, 37-47.

Mayer, B., Kylling, A., Emde, C., Hamann, U., Buras, R., 2011. libRadtran user's guide. http://www.libradtran.org/doc/libRadtran.pdf, last accessed June 2017.

Mayo-Bean, K., Moran, K., Meylan, B., Ranslow, P., 2012. Methodology Document for the ECOlogical Structure-Activity Relationship Model (ECOSAR) Class Program. US-EPA, Washington DC, 46 pp.

McNeill, K., Canonica, S., 2016. Triplet state dissolved organic matter in aquatic photochemistry: Reaction mechanisms, substrate scope, and photophysical properties. Environ. Sci.: Processes Impacts 18, 1381-1399.

NIH, 2017. *https://aidsinfo.nih.gov/drugs/448/sulfadiazine/0/patient*, last accessed August 2017.

Norden (http://www.norden.org), 2012. PPCP monitoring in the Nordic Countries – Status Report. Nordic Council of Ministers, Copenhagen, TemaNord 2012:519.

Polesel, F., Andersen, H. R., Trapp, S., Plósz, B. G., 2016. Removal of antibiotics in biological wastewater treatment systems—A critical assessment using the activated sludge modeling framework for xenobiotics (ASM-X). Environ. Sci. Technol. 50, 10316-10334.

R Development Core.Team, 2017. R: A language and environment for statistical computing,. R Foundation for Statistical Computing, Vienna, Austria, https://www.r-project.org.

Remucal, C. K., 2014. The role of indirect photochemical degradation in the environmental fate of pesticides: A review. Environ. Sci.: Processes Impacts 16, 617-625.

Rosario-Ortiz, F. L., Canonica, S., 2016. Probe compounds to assess the photochemical activity of dissolved organic matter. Environ. Sci. Technol. 50, 12532-12547.

Sanli, N., Sanli, S., Ozkan, G., Denizli, A., 2010. Determination of pK(a) values of some sulfonamides by LC and LC-PDA methods in acetonitrile-water binary mixtures. J. Brazil. Chem. Soc. 21, 1952-1960.

Sobek, S., Tranvik, L. J., Prairie, Y. T., Kortelainen, P., Cole, J. J., 2007. Patterns and regulation of dissolved organic carbon: An analysis of 7,500 widely distributed lakes. Limnol. Oceanogr. *58*, 1208–1219.

Solomon, C. T., Jones, S. E., Weidel, B. C., Buffam, I., Fork, M. L., Karlsson, J., Larsen, S., Lennon, J. T., Read, J. S., Sadro, S., Saros J. E., 2015. Ecosystem consequences of changing inputs of terrestrial dissolved organic matter to lakes: Current knowledge and future challenges. Ecosystems 18, 376-389.

Sun, M., Chang, Z. Q., Van den Brink, P. J., Li, J., Zhao, F. Z., Rico, A., 2016. Environmental and human health risks of antimicrobials used in Fenneropenaeus chinensis aquaculture production in China. Environ. Sci. Pollut. Res. 23, 15689-15702.

Tentscher, P.R., Eustis, S.N., McNeill, K., Arey, J.S., 2013. Aqueous oxidation of sulfonamide antibiotics: aromatic nucleophilic substitution of an aniline radical cation. Chem. Eur. J. 19, 11216-11223.

Vione, D., Minella, M., Maurino, V., Minero, C., 2014. Indirect photochemistry in sunlit surface waters: Photoinduced production of reactive transient species. Chemistry Eur. J. 20, 10590-10606.

Vione, D., Fabbri, D., Minella, M., Canonica, S., 2018. Effects of the antioxidant moieties of dissolved organic matter on triplet-sensitized phototransformation processes: Implications for the photochemical modeling of sulfadiazine. Water Res. 128, 38-48.

Warneck, P., Wurzinger, C., 1988. Product quantum yields for the 305-nm photodecomposition of nitrate in aqueous solution. J. Phys. Chem. 92, 6278-6283.

Wenk, J., Canonica, S., 2012. Phenolic antioxidants inhibit the triplet-induced transformation of anilines and sulfonamide antibiotics in aqueous solution. Environ. Sci. Technol. 46, 5455-5462.

Wenk, J., von gunten, U., Canonica, S., 2012. Effect of dissolved organic matter on the transformation of contaminants induced by excited triplet states and the hydroxyl radical. Environ. Sci. Technol. 45,1334-1340.

Wenk, J., Eustis, S. N., McNeill, K., Canonica, S., 2013. Quenching of excited triplet states by dissolved natural organic matter. Environ. Sci. Technol. 47, 12802-12810.

Wetzel, R. G., 2001. Limnology fof ake and River Ecosystems, 3rd edn., Academic Press, New York.

Weyhenmeyer, G. A., Müller, R. A., Normanm M., Tranvik, L. J., 2016. Sensitivity of freshwaters to browning in response to future climate change. Clim. Change 134, 225-239.

Wilkinson, F., Brummer, J., 1981. Rate constants for the decay and reactions of the lowest electronically excited singlet-state of molecular oxygen in solution, J. Phys. Chem. Ref. Data 10, 809-1000.

Zou, H., Radke, M., Kierkegaard, A., MacLeod, M., McLachlan, M. S., 2015a. Using chemical benchmarking to determine the persistence of chemicals in a Swedish lake. Environ. Sci. Technol. 49, 1646–1653.

Zou, H., Radke, M., Kierkegaard, A., McLachlan, M. S., 2015b. Temporal variation of chemical persistence in a Swedish lake assessed by benchmarking. Environ. Sci. Technol. 49, 9881–9888.